Science of the Total Environment 530–531 (2015) 28–37

Contents lists available at ScienceDirect

Science of the Total Environment

journal homepage: www.elsevier.com/locate/scitotenv

An integrated approach using high time-resolved tools to study the origin of aerosols

A. Di Gilio [a,b], G. de Gennaro [a,b,*], P. Dambruoso [a,b], G. Ventrella [a]

[a] Chemistry Department, University of Bari, via Orabona, 4, 70126 Bari, Italy
[b] ARPA PUGLIA, Corso Trieste, 27, 70126 Bari, Italy

HIGHLIGHTS

- An integrated approach was developed to characterize local and LRT contributions to PM.
- The use of high time-resolved tools allowed one to identify also time-limited events.
- Hourly ion concentrations enabled an accurate characterization of high-PM events.
- Hourly BT cluster analysis enabled the identification of the LRT pathways.
- This approach is useful to understand air pollution phenomena and support decision making.

ARTICLE INFO

Article history:
Received 21 January 2015
Received in revised form 2 April 2015
Accepted 20 April 2015
Available online xxxx

Editor: D. Barcelo

Keywords:
PM2.5
Ambient Ion Monitor (AIM)
Real-time measurements
Anthropogenic long-range transport
Back-trajectory cluster analysis
Hourly ionic composition

ABSTRACT

Long-range transport of natural and/or anthropogenic particles can contribute significantly to PM10 and PM2.5 concentrations and some European cities often fail to comply with PM daily limit values due to the additional impact of particles from remote sources. For this reason, reliable methodologies to identify long-range transport (LRT) events would be useful to better understand air pollution phenomena and support proper decision-making.

This study explores the potential of an integrated and high time-resolved monitoring approach for the identification and characterization of local, regional and long-range transport events of high PM. In particular, the goal of this work was also the identification of time-limited event. For this purpose, a high time-resolved monitoring campaign was carried out at an urban background site in Bari (southern Italy) for about 20 days (1st–20th October 2011). The integration of collected data as the hourly measurements of inorganic ions in $PM_{2.5}$ and their gas precursors and of the natural radioactivity, in addition to the analyses of aerosol maps and hourly back trajectories (BT), provided useful information for the identification and chemical characterization of local sources and trans-boundary intrusions. Non-sea salt (nss) sulfate levels were found to increase when air masses came from northeastern Europe and higher dispersive conditions of the atmosphere were detected. Instead, higher nitrate and lower nss-sulfate concentrations were registered in correspondence with air mass stagnation and attributed to local traffic source. In some cases, combinations of local and trans-boundary sources were observed. Finally, statistical investigations such as the principal component analysis (PCA) applied on hourly ion concentrations and the cluster analyses, the Potential Source Contribution Function (PSCF) and the Concentration Weighted Trajectory (CWT) models computed on hourly back-trajectories enabled to complete a cognitive framework and confirm the influence of aerosol transported from heavily polluted areas on the receptor site.

1. Introduction

Developing appropriate control strategies for air quality involves an understanding of the physical and chemical processes that affect the formation and chemical composition of PM as well as the evaluation of PM transport and mixing processes. Locally emitted pollutants are not only diluted with ambient air but also undergo various types of transformations in the atmosphere. Moreover, natural and anthropogenic aerosol components released at one location can travel long distances in the atmosphere depending on the prevailing weather conditions, which change daily. Thus, PM can affect both local and distant air quality. Evidence suggests that long-range transport (LRT) of PM over distances exceeding natural borders may affect air quality in urban and rural areas throughout

* Corresponding author at: Chemistry Department, University of Bari, via Orabona, 4, 70126 Bari, Italy.
E-mail address: gianluigi.degennaro@uniba.it (G. de Gennaro).

http://dx.doi.org/10.1016/j.scitotenv.2015.04.073
0048-9697/

Europe (Abdalmogith and Harrison, 2005; Niemi et al., 2009; Baker, 2010; M.J. Kim et al., 2012; Gao et al., 2012; Moroni et al., 2012).

The most important meteorological factors influencing air pollution concentrations are atmospheric stratification, dispersive capacity of the atmosphere, high convective dynamics, wind speeds, meteorological conditions, topography and solar radiation (Valkama and Kukkonen, 2004). In different Megacities all over northern Europe as well as in northern Italy, air quality is greatly affected by anthropogenic emissions. Evidence suggests that air pollution problems are principally due to unfavorable weather conditions and orographic features which reduce air mass circulation and favor pollutant accumulation (Lenschow et al., 2001; Putaud et al., 2004; Viana et al., 2006; Carbone et al., 2010; Squizzato et al., 2012). In fact, PM concentrations are highly seasonal and reach their maximum levels in winter, when a lower disperdent capacity of the atmosphere is registered. On the contrary, countries bordering the Mediterranean basin are characterized by a higher planetary boundary layer, especially in summer. This situation sometimes causes an inverse seasonality of PM concentrations due to LRT contributions to local PM levels (Katragkou et al., 2009). These LRT contributions may significantly enhance PM10 levels producing mass loads greater than the European Commission (EC) limit value of 50 μg m^{-3}, especially during the summer season (Bonasoni et al., 2004; Querol et al., 2004; Cristofanelli and Bonasoni, 2009; Escudero et al., 2007; Meloni et al., 2008; Perrino et al., 2009; Riccio et al., 2009; Remoundaki et al., 2011; Nava et al., 2012). Because countries bordering the Mediterranean basin are often downwind from African mineral dust plumes, the most commonly discussed LRT contribution is the Saharan dust transport. In fact, in the guidelines provided by the European Commission (671/11, 2011), Member States are instructed to subtract the contribution of natural sources before comparing PM10 concentrations to the established limits.

However, recent studies have noted an influence from the European continent and suggest that there is also an anthropogenic LRT contribution which can produce an increase in finer particle concentrations for compounds such as sulfate and organic carbon (Glavas et al., 2008; Marenco et al., 2006; Riccio et al., 2007; C.H. Kim et al., 2012; Tositti et al., 2013).

The few work conducted on this issue in the Apulia region of southern Italy, report a non-seasonality for PM concentrations with high values in more dispersive conditions of atmosphere and the ammonium sulfate concentrations homogenously distributed in time and space (Amodio et al., 2010, 2011, 2012). Even if these evidences could exclude the local character of ammonium sulfate, more relevant and time-resolved information could be needed for the identification of anthropogenic LRT events.

Therefore in this study an integrated and high time-resolved monitoring approach was carried out in order to enable the discrimination and the chemical characterization of different sources of PM as well as the identification of LRT events, also time limited. Simultaneously the PM10 and PM2.5 sampling, a high time-resolved monitoring campaign was conducted at an urban background site in Bari (southern Italy) for about 20 days (1st–20th October 2011). This campaign enabled to collect hourly information about the dispersion properties in the lower layers of the atmosphere and about the concentrations of ions in PM2.5 and of their gas precursors in ambient air. Finally, statistical investigations such as the principal component analysis (PCA) applied on these hourly data and the cluster analyses, the Potential Source Contribution Function (PSCF) and the Concentration Weighted Trajectory (CWT) models computed on hourly back-trajectories enabled to complete a cognitive framework necessary for the identification and characterization of LRT events, also short-term.

Identifying the origin of the pollutants and distinguishing between long-range and local contribution could give stakeholders crucial information for the development of cost-effective control strategies and effective abatement measures. In fact, it would help avoid unnecessary air quality control measures such as blocking traffic when atmospheric stability is not determined.

2. Materials and methods

2.1. Integrated monitoring approach

An integrated and high time-resolved monitoring approach was carried out during the campaign performed October 1 to 20, 2011 at an urban background site, located at the Campus of the University of Bari (Lat: 47,1252; Long: 16,6667). This approach integrated PM mass measurements with the hourly information about the dispersion properties in the lower layers of the atmosphere and the hourly concentrations of ions and their gas precursors. In addition, the information obtained by principal component analysis (PCA) applied on hourly data collected and by the statistical models applied to hourly backward trajectories (such as Cluster Analyses, Potential Source Contribution Function (PSCF) and Concentration Weighted Trajectory (CWT)) completed the cognitive framework necessary for the identification and chemical characterization of different contributions to PM, as well as LRT events, also short-term.

2.1.1. PM sampling

The daily PM2.5 and PM10 samples were collected on quartz fiber filters (Whatman, 47 mm diameter) using a dichotomous low volume sampler SWAM Dual Sampler (FAI Instruments S.r.l., Roma, Italy) and FAI EN 1234.1 sampling heads operating at a flow rate of 2.3 m^3 h^{-1}. A total amount of 40 PM2.5 and PM10 samples were collected and stored in a freezer at −4 °C.

2.1.2. Time-resolved characterization of the ionic component of PM2.5 and ionic gaseous precursors

An Ambient Ion Monitor (AIM, URG-9000D, URG Corporation) provided time-resolved direct measurement of cations and anions found in PM2.5 both in particulate (NO_3^-, SO_4^{2-}, Cl^-, NH_4^+, Na^+, K^+, Mg^{2+}, Ca^{2+}, found in PM2.5) and gaseous phases (such as HCl, HNO_3, HNO_2, SO_2 and NH_3). The AIM separated and analyzed each ion individually by incorporating the proven analysis method of ion chromatography. In detail, the instrument consisted of a particle collection unit and two ion chromatograph analyzers for cation and anion analyses. Atmospheric aerosol was sampled at a flow rate of 3 L min^{-1} through a PM2.5 sharp cut cyclone. The air sample was drawn through a liquid diffusion parallel-plate denuder that consisted of two cellulose membranes (one for plate) constantly supplied with a 5 mM H_2O_2(aq) solution, and separated the gas from the aerosol phase. The soluble f were separated from particles by diffusion and dissolution into the denuder solution. At this point, the air flow, free of soluble gases, passed through the denuder and continued into the particle supersaturation chamber. Here the particle hygroscopic growth into droplets was favored in order to achieve high collection efficiencies.

Then the water-soluble components both in their particle and gaseous phase were collected by four 5 ml-syringes (particle and gaseous phases, cation and anion analyses) loaded into pre-concentrators and then injected automatically by a collector into the two ICs once per hour. Each analyzer (ICS-1100, Dionex Corporation, Sunnyvale, CA) was equipped with a guard column (IonPac CG12A, 5 μm, 2 × 50 mm for cations and IonPac AG14A, 4 × 50 mm for anions), an analytical column (IonPac CS12A, 5 μm, 2× 250 mm for cations and IonPac AS14A, 4 × 250 mm for anions), and a self-regenerating suppressor (CSRS 300, 2 mm for cations and ASRS 300, 4 mm for anions). The cation analyzer operated in 15 min isocratic elution with 20 mM methanesulphonic at a flow rate of 0.25 mL/min, whereas the anion analysis was performed in a 27 min isocratic elution with 8 mM sodium carbonate/1 mM sodium bicarbonate at a flow rate of 0.6 mL/min. Multi-point calibrations were performed bi-weekly for both ICs by using calibration

standard solutions (Dionex Corporation, Six Cation-II standard for cation and seven anion standard for anion).

Moreover, it should be noted that the expected collection efficiency of the AIM is considered about 99%, according to the manufacturer (Simon and Dasgupta, 1993). All the LODs for anions and cation were lower than 0.5 μg/m^3, except Na^+ and K^+ which show LODs of about 0.8 μg/m^3.

In addition, NOx concentrations were downloaded from the Regional Agency for Environmental Protection web site (www.arpapuglia.it) where all the data collected by an air quality monitoring network in the Apulia Region are stored. In particular, in this study we utilized the NOx data collected for the monitoring station called 'Politecnico' which is located in the Campus site at the University of Bari.

2.1.3. Meteorological parameter and aerosol maps

Meteorological data such as wind speed (WV), air temperature (T) and barometric pressure (P) were continuously recorded by an automated weather station located in the Campus site at the University of Bari. Moreover, the dispersive capacity of the atmosphere was determined with a PBL Mixing Monitor (FAI Instruments), a sequential automatic system which provides the natural radioactivity counts by measuring Radon decay products with 1-h time resolution. The atmospheric Radon concentration depends on the vertical dilution factor and the Radon products can be considered as natural tracers of the low PBL layer mixing properties. Sulfate and smoke concentration distributions were evaluated using NAAPS (Navy Aerosol Analysis and Prediction System) aerosol maps (http://www.nrlmry.navy.mil/aerosol/) which combine the current and expected satellite data streams with other available data and the global aerosol simulation and prediction (Pérez et al., 2006a,b; Basart et al., 2012).

2.1.4. Principal component analysis (PCA)

Principal component analysis (PCA) has been widely used to identify the pollution sources observed at a receptor site (Amodio et al., 2010; Andriani et al., 2010; Hellebust et al., 2010; Pant and Harrison, 2012). The purpose of PCA is to reduce the number of variables which explain the total variance in the data: it can be obtained by creating new orthogonal and uncorrelated variables, called principal components (PCs), that are linear combinations of the original variables. The first PC explains the largest amount of variance in the original data and each of the subsequent PCs accounts for a lesser fraction of original data variability. The first step of the procedure consists in calculating eigenvalues and eigenvectors of the correlation data matrix; the eigenvectors are rotated in order to obtain a clear pattern of loadings, that is, factors that are somehow clearly marked by high loadings for some variables and low loadings for others. In this work, in order to obtain information on the most relevant emission sources and to distinguish among local and LRT contribution, PCA with Varimax rotation was applied to the hourly concentrations of the ions (such as NO_3^-, SO_4^{2-}, Cl^-, NH_4^+, Na^+, K^+, Mg^{2+}, Ca^{2+}) and their gas precursors (HCl, SO_2, HONO, HNO_3, NOx and NH_3), determined by AIM900D from the 1st to 20th October 2011.

2.1.5. Backtrajectory statistical models

Analytical back-trajectories (BTs) of air masses provide information about the origin of the aerosols observed at a particular location and on the dynamical patterns governing this transport of air masses. Therefore, BTs computed from archived meteorological data, can be useful in identifying the origins of pollutants measured at a receptor site. Air mass BTs were calculated using NOAA Hybrid Single Particle Lagrangian Integrated Trajectory transport model (HYSPLIT 4.9) (Draxler and Rolph, 2003) and employing archived meteorological data supplied by the NOAA/ARL (Air Resources Lab, http://ready.arl.noaa.gov/gdas1.php) and global data assimilation system (GDAS1). In order to characterize the general behavior of air masses in a given sampling period and to evaluate the relative contributions by local sources and long range intrusions to the total PM, 4-day BTs were run hourly at three endpoints located at 750, 1500 and 2500 m a.g.l.

Then, the cluster analysis package included in the 4.9 version of HYSPLIT characterized the ensemble of 481 calculated four-day BTs terminating at a height of 750 m a.g.l. and recorded every hour during the study period. The 4-day BTs were utilized as input variables for the K-means clustering algorithm and the distances between trajectories were computed using simple Euclidean distance. Next, a cluster analysis algorithm was used to categorize the computed trajectories into groups of similar properties, the so-called clusters. The average BT of each cluster was then calculated from its trajectory members. Since accuracy in BT calculation decreases with distance and time (due to model assumptions and spatial and temporal resolution of the meteorological data), 4-day trajectories were considered the most suitable option. Moreover, the clustering of BTs reduced errors associated with single trajectories. Finally, in order to confirm the long range transport contribution to PM locally measured and to localize the source emission, two statistical models were applied to 4-day-backtrajectories at 750 m.a.s.l. starting point: Potential Source Contribution Function (PSCF) and Concentration Weighted Trajectory (CWT). The first one depends on the frequency of passages over each grid cell for trajectories associated to concentrations above a specified quantile (90th for this study) therefore it calculates the probability that a source is located at latitude *i* and longitude j. The CWT computes a logarithmic mean of concentration at the receptor weighted by the residence time of the trajectory for each grid cell of the geographical domain (Cheng et al., 2013; Fleming et al., 2012; Carslaw and Ropkins, 2012; Wang et al., 2012). These statistical data analyses have been performed within the software environment R 3.0.2 (R Development Core Team, 2013).

3. Results and discussion

3.1. Identification and characterization of high-PM events

In order to identify the different contributions affecting PM levels in the Apulia region, hourly concentrations of water-soluble ions and their precursor gases were collected between October 1 and 20, 2011 at urban background site at the Campus location of the University of Bari. The data collected was integrated with information about the diffusive properties of the low layers of the atmosphere and information provided by aerosol maps and BTs. During the sampling period, the mean PM10 and PM2.5 concentrations were 49.5 μg/m^3 and 26.2 μg/m^3, respectively, and the 90.4 percentile of PM10 concentrations (66.4 μg/m^3) exceeded the concentration limit established by European Directive (2008/50/CE). Moreover, during the twenty sampling days, PM10 concentrations exceeded the daily limit value (50 μg/m^3) for eleven days (Fig. 1).

In particular, as shown in Fig. 1, high PM concentrations were registered in days characterized by the atmospheric stability, which determined the accumulation of air pollutants locally emitted. Only one exception it was possible to consider: the period from 10th to 11th October was characterized by high PM concentrations and the lowest values of natural radioactivity counts.

In the monitoring period, the mean nitrate and nitrite concentrations (0.40 and 0.37 μg/m^3, respectively) accounted for 6.1% and 5.6% to the total ion concentration, respectively (Table 1), and they were strongly correlated with NOx and the natural radioactivity counts (Fig. 2). The mean value of nitrogen oxidation ratio (NOR) defined as $NOR = nNO_3^-/(nNO_3^- + nNO_2)$ was 0.6 ± 0.2 and the highest values were registered in correspondence of atmospheric stability and high relative humidity that favored the gas-to-particle conversion processes. The same feature was not obtained for nss-sulfate (calculated indirectly using the seawater ratio ($nss\text{-}SO_4^{2-} = SO_4^{2-} - 0.25 * Na^+$) accounting for 36% of the total ion concentration. In the monitoring period, the mean of hourly nss-sulfate mean concentrations was 2.43 μg/m^3 (Table 1) and the mean sulfate oxidation ratio (SOR), defined as $SOR = nSO_4^{2-}/$

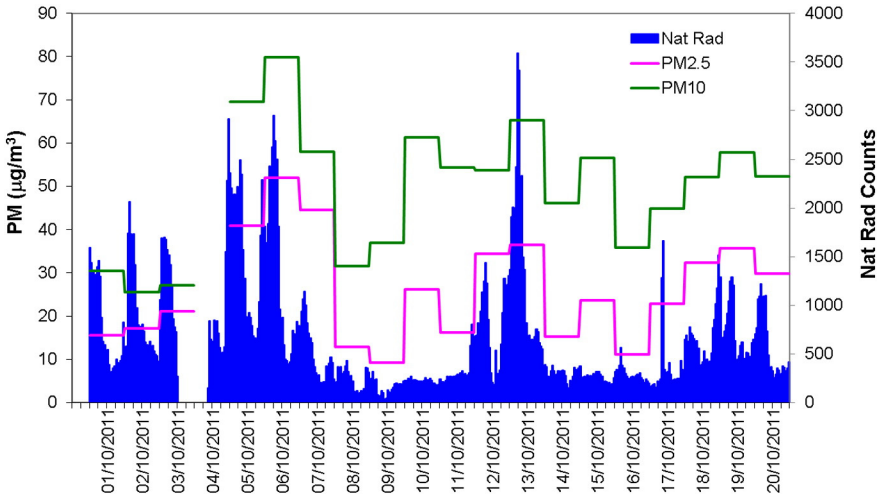

Fig. 1. PM2.5 and PM10 concentrations (µg/m^3) and natural radioactivity counts.

Table 1
Mean, maximum (Max) and minimum (Min) values of the hourly concentrations of ions and their gas precursors and mean percentage concentrations for each ion with respect to the total ionic composition (%).

	Monitoring period				October, from 12 to 13 and from 18 to 20				October, from 5 to 7				October, from 10 to 11			
µg/m^3	Mean	Max	Min	%	Mean	Max	Min	%	Mean	Max	Min	%	Mean	Max	Min	%
nss-SO_4^{2-}	2.43	9.16	0.17	36	1.75	4.40	0.39	26	3.28	4.12	2.02	38	2.61	9.16	0.77	58
NO_3^-	0.40	2.42	0.05	6.1	0.44	2.18	0.14	6.4	0.54	1.95	0.11	6.2	0.27	0.87	0.07	6.0
Cl^-	0.17	1.71	0.01	2.6	0.18	1.71	0.01	2.6	0.08	0.29	0.01	0.9	0.25	0.44	0.04	5.5
NO_2^-	0.37	1.99	0.01	5.6	0.48	1.71	0.02	7.1	0.53	1.99	0.10	6.2	0.13	0.69	0.03	2.8
K^+	0.08	1.18	0.01	1.2	0.12	1.18	0.01	1.8	0.13	0.44	0.03	1.5	0.01	0.06	0.01	0.3
Mg^{2+}	0.01	0.10	0.01	0.2	0.01	0.06	0.01	0.1	0.01	0.01	0.01	0.1	0.03	0.10	0.01	0.6
Ca^{2+}	0.07	3.44	0.01	1.1	0.12	3.44	0.01	1.8	0.11	0.44	0.03	1.3	0.03	0.08	0.02	0.7
Na^+	0.32	3.60	0.05	4.8	0.32	2.69	0.05	4.6	0.26	1.96	0.10	3.0	0.57	2.03	0.22	13
NH_4^+	2.80	6.67	0.05	42	3.45	6.67	0.18	50	3.72	5.86	1.88	43	0.63	1.53	0.05	14
SO_2	2.04	36.07	0.0		1.36	5.15	0.04		1.68	13.03	0.01		1.32	6.44	0.17	
HNO_3	0.32	5.54	0.06		0.23	3.41	0.06		0.27	0.74	0.13		0.13	0.32	0.08	
HCl	0.25	2.42	0.01		0.28	1.94	0.11		0.22	0.58	0.06		0.19	0.50	0.01	
HONO	0.21	2.01	0.01		0.33	2.01	0.01		0.21	1.00	0.01		0.05	0.66	0.01	
NH_3	1.57	8.58	0.18		0.94	2.33	0.30		2.91	7.99	1.62		0.99	2.08	0.41	

($nSO_4^{2-} + nSO_2$), was 0.61 ± 0.04, suggesting the occurrence of secondary aerosol in Bari. Several studies, in fact, reported that SOR is less than 0.25 for primary pollutants while the chemical oxidation of SO_2 would occur in the atmosphere when SOR is greater than 0.25 (Li et al., 2013; Ohta and Okita, 1990; Wang et al., 2005). However high SO_2 concentrations were registered when higher dispersive atmospheric conditions occurred and the uncorrelated behaviors of nss-sulfate and SO_2 hourly concentrations were registered (Fig. 3). These results suggested that the secondary nss-sulfate was not due to oxidation of SO_2 locally emitted but it came from across-boundary transport. Therefore a mixing and smoothing of sulfate in wider region in South of Italy were determined (Li et al., 2013).

In order to deepen the causes of the high PM events, the attention was paid on the exceedance days and the data analysis resulted in the

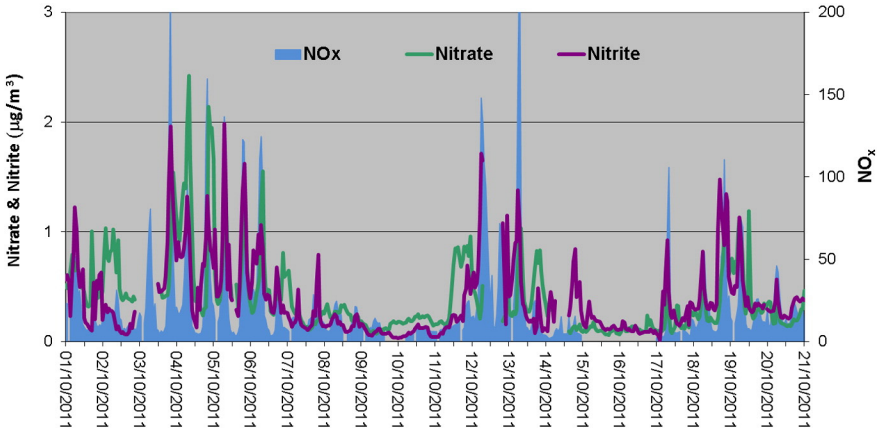

Fig. 2. Trend of NO_3^-, NO_2^- and NO_x hourly concentrations.

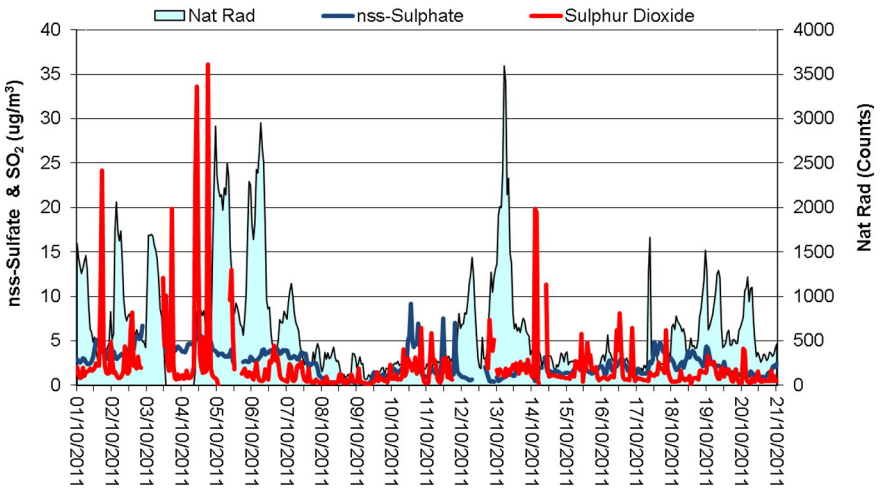

Fig. 3. Trend of nss-SO_4^{2-} and SO_2 hourly concentrations.

integration of different information: the PM2.5/PM10 ratio, the natural radioactivity counts, the meteorological data, the hourly concentrations of ions and their precursor gases and the information provided by aerosol maps and backtrajectories. In this way, among the PM exceedance days, it has been possible to distinguish the following high PM events:

- Local event (exceedance days from October 12 to 13 and from 18 to 20);
- Anthropogenic LRT event (exceedance days from October 10 to 11);
- Event due to the synergistic effect of local and eastern Europe contributions (exceedance days from October 5 to 7).

The exceedance days from October 12 to 13 and 18 to 20 showed a mean PM2.5/PM10 ratio equal to 0.6 and high values of natural radioactivity counts. In these dates, atmospheric stability determined the accumulation of air pollutants locally emitted and a significant fine contribution to PM concentrations. The hourly mean concentrations of nitrate and nitrite were equal to 0.44 and 0.48 μg/m^3 with maximum values of 2.18 and 1.71 μg/m^3, respectively. These values were about four times higher than mean hourly values observed during the sampling campaign (0.4 and 0.37 μg/m^3, respectively). Moreover the nitrate and nitrite hourly concentrations were strongly correlated to NOx concentrations (Fig. 2), and the correlation coefficient between nitrate and HNO_3 and between nitrite and HONO was equal to 0.90 (Table 2). In these days the highest values of nitrogen oxidation ratio were registered (NOR ranging from 0.4 to 1) suggesting that a considerable secondary nitrate formation from NOx occurred. Nitrate and nitrite are typical markers of traffic source because their formation is usually favored by the availability of nitric acid, which forms from gaseous precursors as nitrogen oxides (NOx). These compounds are produced by combustion processes and occur in engines where high temperatures are reached; therefore, their concentrations in the air can be largely associated with vehicle transport emissions (M.J. Kim et al., 2012; Masiol et al., 2012). Moreover in this period the nss-sulfate concentrations accounted for 26% of the total ion concentration and the mean values of nss-SO_4 and SO_2 were equal to 1.75 and 1.36 μg/m^3, respectively. They were lower than the mean values determined over the monitoring campaign (2.43 and 2.04 μg/m^3, respectively) and the mean molar ratio of NH_4^+ to SO_4^{2-} greater than 2, suggested the complete neutralization of H_2SO_4 by NH_3 and an excess of NH_3 in atmosphere. The average molar ratio for NH_4^+ to the sum of SO_4^{2-}, NO_3^-, NO_2^- and Cl^- was 3.2, indicating that an appreciable amount of NH_4^+ contributed from salts of carbonic acid such as $(NH_4)_2CO_3$ and NH_4HCO_3 and salts of organic acids CH_3COONH_4 and $HCOONH_4$.

Moreover, in this period, the mean sulfate oxidation ratio was 0.59 and decreased to 0.38 with minimum value of 0.07 (in night hours) from October 12 to 13. The mean NOR value (0.68) higher than SOR value suggested that the secondary formation of sulfate from SO_2 weakly occurred in comparison to that of NO_3 from NOx. In fact, in these days, the secondary aerosol was characterized by ammonium nitrate rather than ammonium sulfate. In addition, the aerosol maps did not show significant concentrations of sulfate at the sampling site, and BTs suggested a local recirculation of air masses. All these results suggested a local contribution to PM exceedances due to vehicular traffic.

During the exceedance days from October 10 to 11, the day–night profile of natural radioactivity was less evident because of more dispersive atmospheric conditions, however, PM10 concentration on October 10 and 11 reached values similar to those during the other exceedance days. The PM2.5/PM10 ratio on these days was equal to 0.3 showing a coarse contribution to the PM concentration. The local contribution to PM concentration was excluded due to the lower concentrations of NH_4^+, NO_3^-, NO_2^- and NO_x during these days. Nevertheless, the highest levels of nss-sulfate hourly concentrations (max value: 9.16 μg/m^3) were registered in these date when this pollutant accounted for 58% of the total ion concentration. Moreover the mean SOR was equal to 0.6 suggesting a noticeable contribution of secondary nss-sulfate to PM, but in correspondence of SO_2 hourly concentrations similar to those registered from 12 to 13 and from 18 to 20 October, the highest nss-sulfate concentrations were probably due to long range transport carrying secondary sulfate from remote area (Squizzato et al., 2012; Li et al., 2013). Moreover, unlike other monitoring period, the ionic balance on these days showed a higher anionic contribution and the equivalent ratio between NH_4^+ and the sum of $SO_4^{2-} + NO_3 + NO_2$ gave a value lower than 1 (ratio = 0.57) indicating the existence of another neutralizing agent in addition to ammonia. In fact, the charge balance between cations, i.e. sum of NH_4^+, K^+, Na^+, Ca^{2+} and Mg^{2+} and anions, i.e. sum of Cl^-, NO_3^-, and SO_4^{2-} was closer to 1:1 line (ratio = 0.93). It may be that during the long range transport, H_2SO_4 reacted with different basic species or other salts. These results may be confirmed, for example, by the correlation coefficients between nss-sulfate and calcium (Corr. Coef equal to 0.80) and magnesium (Corr. Coef = 0.71) (Table 2) and by the trends of calcium and nss-sulfate on these days (Koçak et al., 2004) (Fig. 4 insert). Finally, the information provided by BTs highlighted the intrusion of an air mass from northeastern Europe over the southern regions of Italy and the sulfate concentrations provided by the aerosol maps were consistent with those determined by AIM instrumentation. All these results suggested an anthropogenic LRT contribution to PM exceedances.

Table 2
Correlation coefficient among hourly concentrations of ions and their gas precursors for the three high PM events.

October, from 12 to 13 and from 18 to 20	NO_3^-	Cl^-	NO_2^-	K^+	Mg^{2+}	Ca^{2+}	Na^+	NH_4^+	SO_2	HNO_3	HCl	HNO_2	NH_3
SO_4^{2-}	0.10	0.15	−0.01	−0.06	−0.33	−0.06	−0.32	0.50	0.40	−0.25	−0.16	−0.39	−0.16
NO_3^-		0.07	0.08	0.44	0.18	0.09	0.01	0.70	0.28	0.90	0.07	0.22	−0.06
Cl^-			−0.05	0.65	0.22	0.65	−0.21	0.36	−0.15	−0.10	−0.11	−0.23	0.13
NO_2^-				0.01	0.08	−0.02	0.15	0.05	0.07	0.15	0.14	0.90	−0.35
K^+					0.63	0.81	0.41	−0.51	0.15	−0.02	−0.10	0.35	−0.21
Mg^{2+}						0.61	0.80	−0.80	0.38	0.34	0.24	0.67	−0.28
Ca^{2+}							0.51	−0.50	0.10	0.10	0.05	0.14	0.04
Na^+								−0.67	0.30	0.10	0.06	0.15	−0.42
NH_4^+									−0.43	−0.34	−0.24	−0.78	0.40
SO_2										0.60	0.67	0.57	0.23
HNO_3											0.94	0.58	0.34
HCl												0.49	0.42
HNO_2													−0.39

October, from 5 to 7	NO_3^-	Cl^-	NO_2^-	K^+	Mg^{2+}	Ca^{2+}	Na^+	NH_4^+	SO_2	HNO_3	HCl	HNO_2	NH_3
SO_4^{2-}	0.33	0.27	−0.05	0.38	0.05	0.05	−0.10	0.58	0.20	0.31	−0.02	0.11	0.31
NO_3		0.54	0.63	0.58	0.64	0.49	−0.16	0.66	−0.03	−0.09	−0.52	0.71	0.06
Cl^-			0.30	0.41	0.20	0.23	0.06	0.35	−0.19	−0.18	−0.27	0.29	−0.13
NO_2^-				0.36	0.74	0.72	−0.03	0.36	0.06	0.02	−0.50	0.52	0.04
K^+					0.21	0.41	−0.24	0.45	0.06	0.18	−0.29	0.36	0.15
Mg^{2+}						0.70	−0.26	0.47	0.16	−0.03	−0.41	0.65	0.10
Ca^{2+}							−0.16	0.37	0.40	0.19	−0.23	0.30	0.24
Na^+								−0.42	−0.11	−0.16	−0.20	−0.23	−0.07
NH_4^+									−0.11	−0.03	−0.32	0.30	0.02
SO_2										0.75	0.48	0.07	0.91
HNO_3											0.64	0.08	0.71
HCl												−0.33	0.37
HNO_2													0.18

October, from 10 to 11	NO_3^-	Cl^-	NO_2^-	K^+	Mg^{2+}	Ca^{2+}	Na^+	NH_4^+	SO_2	HNO_3	HCl	HNO_2	NH_3
SO_4^{2-}	0.27	0.27	0.32	0.50	0.71	0.80	0.13	0.62	−0.01	−0.11	0.05	0.25	−0.48
NO_3		0.32	0.78	0.60	0.59	0.49	−0.04	0.49	0.23	0.40	0.45	0.49	−0.22
Cl^-			−0.05	0.06	0.70	0.24	0.24	0.21	0.20	0.12	0.22	0.20	−0.61
NO_2^-				0.63	0.32	0.48	−0.04	0.31	0.14	0.20	0.21	0.45	0.05
K^+					0.41	0.55	0.12	0.66	0.34	0.02	0.22	0.13	−0.36
Mg^{2+}						0.72	0.08	0.48	0.25	0.10	0.26	0.29	−0.59
Ca^{2+}							0.22	0.49	0.20	−0.06	0.01	0.26	−0.21
Na^+								−0.20	−0.07	−0.11	−0.15	−0.03	0.05
NH_4^+									0.48	0.15	0.38	0.16	−0.64
SO_2										0.63	0.69	0.24	−0.30
HNO_3											0.89	0.25	0.10
HCl												0.23	−0.20
HNO_2													0.04

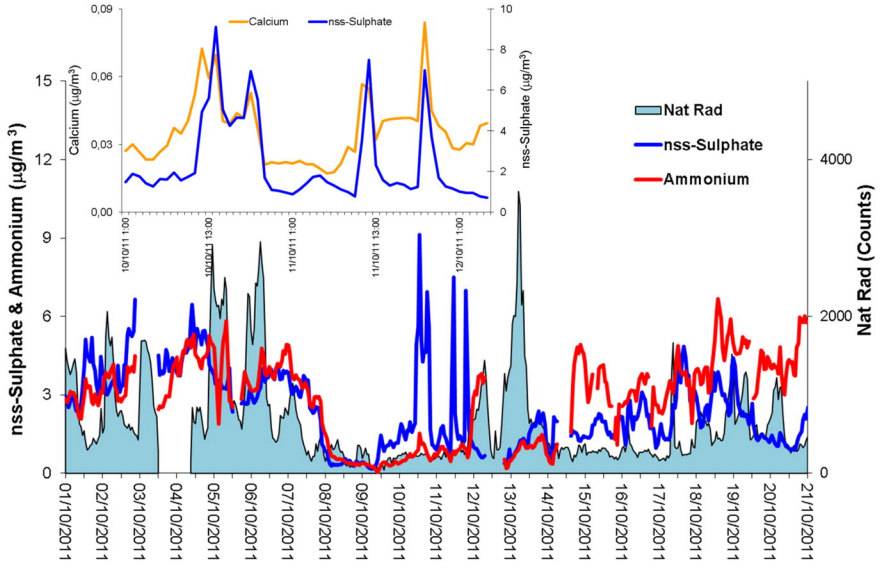

Fig. 4. Trend of nss-SO_4^{2-} and NH_4^+ hourly concentrations for entire sampling period and Ca^{2+} hourly concentrations during a three-day period (inset).

From October 5 to 7 the PM20.5/PM10 ratio was equal to 0.8 indicating an important fine particle contribution to the PM concentrations. The natural radioactivity counts and the mean concentrations of nitrate and nitrite were similar to those determined on October 12–13 and 18–20, but also high concentrations of ammonium sulfate were determined (Fig. 4). On these days, the mean nss-sulfate concentration was equal to 3.28 μg/m^3 with a maximum value of 4.12 μg/m^3 and accounted for 38% of the total ion concentration. The highest SOR values (mean 0.72) were registered in this period and even if the mean SO_2 concentration was similar to that registered from October 12 to 13 and from 18 to 20, the mean sulfate concentration was about twice. The values of ozone concentrations, temperature and humidity were similar during both periods, suggesting that SO_2 oxidation was not the only responsible of sulfate presence in atmosphere. On these days, aerosol maps and BT information revealed a secondary aerosol contribution to the PM concentrations found at the sampling site, and LRT from eastern Europe. Hence, the PM levels and the sulfate concentrations on October 5–7 were probably the result of a synergic effect of regional and long-range contributions.

3.2. Principal component analysis (PCA)

In order to identify the sources of water-soluble ions in PM2.5 and their gas precursors, principal component analysis (PCA) with the varimax normalized rotation was applied to the normalized data matrix of 403 hourly samples and 15 variables (ions and their gas precursors). The loadings and percentages of the explained variance obtained for each of the components are shown in Table 3. Variable factor loadings were used to identify source profiles and to evaluate anthropogenic and natural contributions at the sampling sites. Only variables with factor loadings greater than 0.5 were taken into account in order to characterize source profiles.

In the monitoring campaign, three principal components were obtained and accounted for 80% of the total variance. The principal component 1 accounted for 36% of the total variance, and showed high loadings for NOx, NO_2^-, NO_3^-, K^+, Ca^{2+}, NH_4^+, NH_3 and HONO, indicating its relation to local emissions and a strong contribution of traffic source. The principal component 2, accounting for 29% of the total variance, was characterized by high loadings for Cl^-, Mg^{2+}, Na^+, HNO_3 and HCl. This PC was associated with the marine contribution. The hourly sample showing high scores for PC2 in fact, were characterized by high wind speed blowing from the sea (North direction) and by lower ammonia concentrations. Moreover the Cl/Na ratio was less than the sea water ratios (1.8) indicating a deficiency of chloride relative to the Na concentration and confirming the chloride depletion due to reaction between HNO_3 and NaCl.

Table 3
Loadings and percentage of explained variance obtained by PCA for ions and their gas precursors.
More relevant loadings are reported in bold and italics

	PC1	PC2	PC3
SO_4^{2-}	***0.3***	−0.5	***0.4***
NO_3^-	***0.7***	−0.1	0.2
Cl^-	0.1	***0.6***	0.01
NO_2^-	***0.8***	−0.2	−0.1
K^+	***0.8***	−0.2	0.2
Mg^{2+}	0.03	***0.8***	0.3
Ca^{2+}	***0.7***	0.1	0.2
Na^+	0.01	***0.7***	−0.01
NH_4^+	***0.5***	−0.6	***0.2***
SO_2	***0.4***	***0.4***	***0.5***
HNO_3	***0.3***	***0.5***	***0.5***
HCl	−0.04	***0.6***	***0.5***
HNO_2	***0.7***	0.3	0.3
NH_3	***0.6***	0.1	***0.5***
NOx	***0.5***	−0.04	−0.5
Variance (%)	**36**	**29**	**15**

The principal component 3 which explained 15% of the total variance, showed high loadings for SO_2, NH_3, HNO_3 and HCl. Moreover the nss-SO_4^{2-} showed about the same loading values for both PC1 and PC3, indicating its association with secondary sulfate aerosols due to local distribution (PC1) and to long-range air-mass transport (PC3). In fact, the local nss-sulfate in PC1 was strongly correlated with traffic marker pollutants (NOx, nitrate, ammonium, etc.) and due to atmospheric stability which determines a locally pollution accumulation. On the contrary nss-sulfate in PC3 was correlated with primary gas pollutants and the PC3 was characterized by high score values when high dispersive atmospheric condition occurred.

3.3. Back trajectory statistical model

LRT appears to play a dominant role in the air pollution in southern Italy. In order to evaluate and confirm the influence of local sources and long range intrusions on the PM concentrations, three-dimensional four-day BTs were computed every hour throughout the sampling period and then a cluster analysis was performed. Upon considering the results of the total spatial variance analysis, the appropriate number of clusters was set at 4. In order to understand the transport characteristics of air masses and their impact on aerosol pollution, the mean transport pathway and the percentage of each identified air mass category were calculated (Fig. 5). The results of BT cluster analyses indicated extensive transport of air masses from northeastern and eastern Europe.

Cluster 1 was the most frequent accounting for 57% of the observations during the sampling period. This cluster included trajectories from northeastern Europe passing over the Balkans, Hungary and Slovakia. Cluster 2 (25%) was characterized by the air masses circulating over southern Italy, while cluster 3 (8%) included the masses characterized by northwesterly flows. Finally, cluster 4 accounted for 10% of the observations during the sampling period and included trajectories coming from eastern Europe passing over Romania, Ukraine and Belarus.

The ionic composition of each air mass cluster was examined by sorting the hourly data on major PM2.5 water-soluble ions. The mean ion concentrations and the natural radioactivity counts for each cluster are shown in Fig. 6. Despite the relative lower natural radioactivity counts and the more dispersive conditions of the atmosphere for cluster 1 with respect to cluster 2, the nssSO_4^{2-} concentration for cluster 1 was higher (Fig. 6a). In fact, this cluster showed the highest concentrations of nssSO_4^{2-} (2.83 μg/m^3). Similarly to the first cluster, cluster 2 was characterized by high concentrations of NO_3^- and NO_2^- and also NH_4^+, Ca^{2+}, $Mg2^+$ and K^+. The high content of crustal species together with the vehicular traffic markers suggested a local contribution to the PM concentrations. However, the nssSO_4^{2-} concentration in cluster 2 was lower than that of cluster 1 (2.1 μg/m^3). Taking into account the lower atmospheric dispersive conditions that allowed the stagnation of pollutants locally emitted, its ionic composition and air mass behavior (Fig. 5), the cluster 2 may be linked to a local contribution or more specifically to an air mass recirculation over southern Italy. On the contrary, a comparison of the characteristics of cluster 1 with those of cluster 2 and a consideration of the air mass trajectory lead to the hypothesis of a synergistic effect of local and eastern Europe contributions.

When higher atmospheric dispersive conditions occurred, instead, lower pollutant concentrations could be expected (cluster 3); in particular, nssSO_4^{2-} concentrations lower than the mean value during the sampling period were registered for this cluster (1.1 μg/m^3), characterized by air masses coming from northern Europe.

Finally, cluster 4 was characterized by high nssSO_4^{2-} concentrations (2.75 μg/m^3 in average) even if higher dispersive conditions were registered. Considering both the information obtained from aerosol modeling which was based on the European emission inventory and the ionic composition of this cluster, an anthropogenic LRT contribution from northeastern Europe may be hypothesized. This cluster, in fact, was characterized by lower nitrate and nitrite concentrations, which are locally emitted pollutants, yet it presented high nss-sulfate concentrations. This

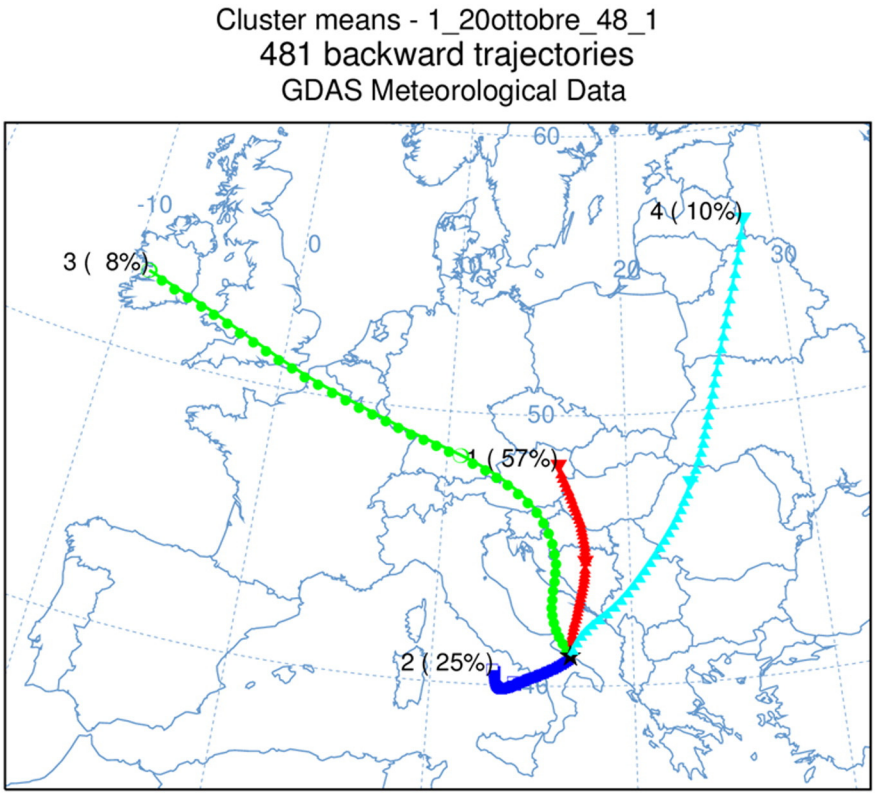

Fig. 5. Representative means of 4-day back-trajectory clusters (inset).

indicates that cluster 4 air masses must have passed over densely populated and highly industrialized regions before arriving at the sampling site. As a result, these air masses may be strongly influenced by anthropogenic pollutions. In particular, in many countries in Eastern Europe (Romania, Ukraine, Poland and Belarus) high SO_2 concentrations are released into the atmosphere from industries using high sulfur fuel (Salvador et al., 2007); and sulfate can be transported long distances due to its stability in the atmosphere (Leck and Persson, 1996).

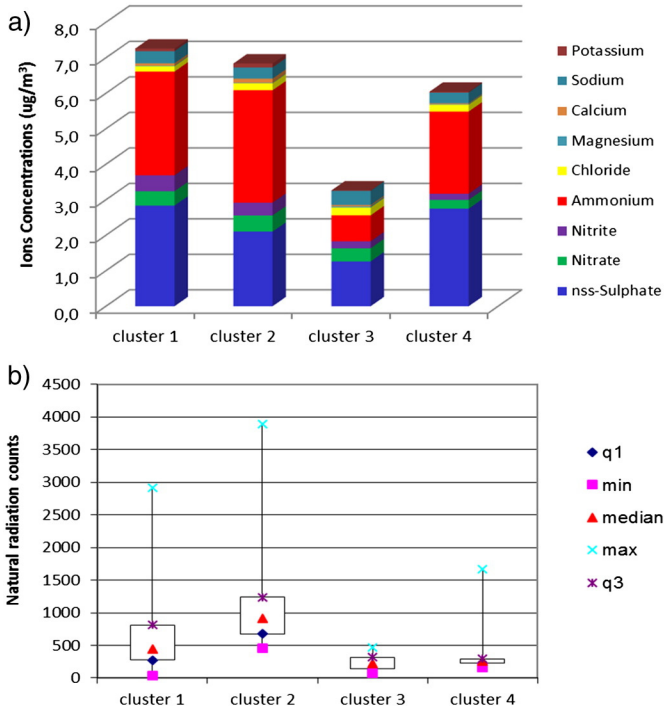

Fig. 6. Ionic composition of PM2.5 (a) and Box-Plot of natural radioactivity counts (b) for each back-trajectory cluster.

In order to confirm the nss-sulfate LTR, other statistical models applied to backtrajectories as PSCF and as CWT models were applied. These models allowed one to provide a comprehensive view of the potential source regions of nss-sulfate in South of Italy. Both statistical models applied to 4 day-backtrajectories by HYSPLIT (GDAS reanalysis meteorological data and 30 m.a.s.l. starting point). The results of PSCF and CWT analysis for nss-sulfate were showed in Fig. 7. The highest PSCF values were obtained for Poland region source, while high weighted concentrations of nss-sulfate were determined through Balkans, Slovachia and Poland. Therefore these models corroborate that the major potential source of this pollutant was located in the North-Est Europe where the location of power plant is consistent for the secondary sulfate source.

4. Conclusions

In this work, an integrated high time-resolved approach was proposed to differentiate between the role of anthropogenic LRT episodes and local sources on PM concentrations and ionic composition. This approach combined hourly PM2.5 ionic composition with hourly information about the properties of the atmosphere and BT statistical analysis. It gives a broad cognitive framework on air quality and, in particular, it allows one to identify and characterize also time-limited transport events.

The result analysis demonstrated that PM concentration levels were predominantly due to both LRT and local atmospheric circulation in the studied area during the period of investigation. High nitrate concentrations occurred in correspondence with a period of stable atmospheric conditions, and could be linked to local sources. The nss-sulfate levels increased when the air mass trajectories moved from northeastern and eastern Europe even if high dispersive conditions of the atmosphere were registered. Occasionally, trans-boundary intrusions of anthropogenic particles were added to those locally emitted.

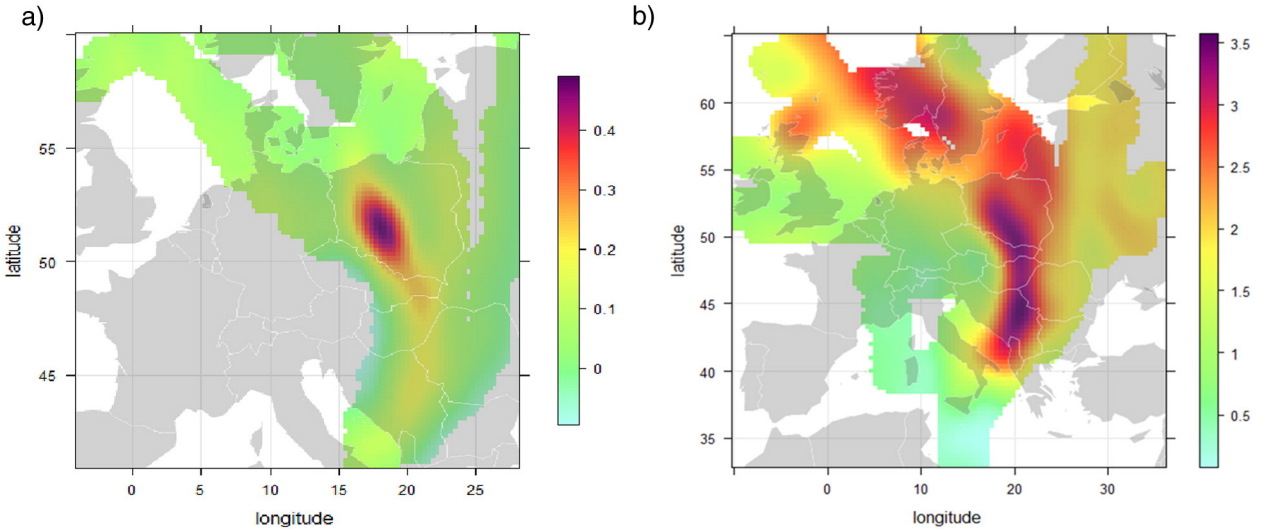

Fig. 7. Spatial distribution of PSCF values (a) of nss-sulfate obtained via combining backward trajectories calculated hourly and hourly samples data set (a). Spatial distribution of weighted concentration of nss-sulfate obtained by the CWT method using hourly measurement data (b).

Moreover, the PCA applied to hourly data allowed one to distinguish among the events characterized by high sulfate concentrations due to local and those caused by an anthropogenic LRT contribution. Finally, statistical models such as Cluster Analysis, the Potential Source Contribution Function (PSCF) and Concentration Weighted Trajectory (CWT), applied to hourly air mass BT and combined with hourly data of ions and their gas precursors, confirmed the influence of time-limited LRT events on receptor site and allowed their chemical characterization.

Finally, this integrated approach highlighted the relevant role of LRT on the PM levels measured in Southern Italy, suggesting that abatement measures should include not only local actions, but also control strategies coordinated at an international level. Further studies will aim to upgrade this integrated monitoring system with a high time-resolved chemical characterization of PM in terms of metals and organic and elemental carbon in order to quantify the different source contributions to PM concentrations.

References

Abdalmogith, S.S., Harrison, R.M., 2005. The use of trajectory cluster analysis to examine the long-range transport of secondary inorganic aerosol in the UK. Atmos. Environ. 39, 6686–6695.

Amodio, M., Andriani, E., Cafagna, I., Caselli, M., Daresta, B.E., de Gennaro, G., Di Gilio, A., Placentino, C.M., Tutino, M., 2010. A statistical investigation about sources of PM in South Italy. Atmos. Res. 98, 207–218.

Amodio, M., Andriani, E., Angiuli, L., Assennato, G., de Gennaro, G., Di Gilio, A., Giua, R., Intini, M., Menegotto, M., Nocioni, A., Palmisani, J., Perrone, M.R., Placentino, C.M., Tutino, M., 2011. Chemical characterization of PM in Apulia Region: local and long-range transport contributions to particulate matter. Boreal Environ. Res. 16, 251–261.

Amodio, M., Andriani, E., Loiotile, Demarinis, de Gennaro, G., Di Gilio, A., Placentino, M.C., 2012. An integrated approach to identify the origin of PM10 exceedances. Environ. Sci. Pollut. Res. 19, 3132–3141.

Andriani, E., Caselli, M., Ielpo, P., de Gennaro, G., Daresta, B.E., Fermo, P., Piazzalunga, A., Placentino, M.C., 2010. Application of CMB model to PM10 data collected in a site of south Italy: results and comparison with APCS model. Curr. Anal. Chem. 6, 19–25.

Baker, J., 2010. A cluster analysis of long range air transport pathways and associated pollutant concentrations within the UK. Atmos. Environ. 44, 563–571.

Basart, S., Pérez, C., Nickovic, S., Cuevas, E., Baldasano, J.M., 2012. Development and evaluation of the BSC-DREAM8b dust regional model over Northern Africa, the Mediterranean and the Middle East. Tellus B 64, 1–23.

Bonasoni, P., Cristofanelli, P., Calzolari, F., Bonafé, U., Evangelisti, F., Stohl, A., Zauli Sajani, S., van Dingenen, R., Colombo, T., Balkanski, Y., 2004. Aerosol-ozone correlations during dust transport episodes. Atmos. Chem. Phys. 4, 1201–1215.

Carbone, C., Decesari, S., Mircea, M., Giulianelli, L., Finessi, E., et al., 2010. Size-resolved aerosol chemical composition over the Italian Peninsula during typical summer and winter conditions. Atmos. Environ. 44, 5269–5278.

Carslaw, D., Ropkins, K., 2012. Openair an R package for air quality data analysis. Environ. Model. Softw. 27–28, 52–61.

Cheng, I., Zhang, L., Blanchard, P., Dalziel, J., Tordon, R., 2013. Concentration-weighted trajectory approach to identifying potential sources of speciated atmospheric mercury at an urban coastal site in Nova Scotia, Canada. Atmos. Chem. Phys. 13, 6031–6048.

Cristofanelli, P., Bonasoni, P., 2009. Background ozone in the southern Europe and Mediterranean area: influence of the transport processes. Environ. Pollut. 157, 1399–1406.

Directive 2008/50/EC of the European Parliament and of the Council of 21 May 2008 on ambient air quality and cleaner air for Europe.

Draxler, R.R., Rolph, G.D., 2003. HYSPLIT (HYbrid Single-Particle Lagrangian Integrated Trajectory). NOAA Air Resources Laboratory, Silver Spring, MD (Model access via NOAA ARL READY Website http://www.arl.noaa.gov/ready/hysplit4.html).

Escudero, M., Querol, X., Avila, A., Cuevas, E., 2007. Origin of the exceedances of the European daily PM limit value in regional background areas of Spain. Atmos. Environ. 41, 730–744.

Fleming, Z.L., Monks, P.S., Manning, A.J., 2012. Review: untangling the influence of air-mass history in interpreting observed atmospheric composition. Atmos. Res. 104105, 1–39.

Gao, X., Xue, L., Wang, X., Wang, T., Yuan, C., Gaao, R., Zhou, Y., Nie, W., Zhang, Q., Wang, W., 2012. Aerosol ionic components at Mt. Heng in central southern China: abundances, size distribution, and impacts of long-range transport. Sci. Total Environ. 433, 498–506.

Glavas, S.D., Nikolakis, P., Ambatzoglou, D., Mihalopoulos, N., 2008. Factors affecting the seasonal variation of mass and ionic composition of PM2.5 at a central Mediterranean coastal site. Atmos. Environ. 42, 5365–5373.

Hellebust, S., Allanic, A., O'Connor, I.P., Wenger, J.C., Sodeau, J.R., 2010. The use of real-time monitoring data to evaluate major sources of airborne particulate matter. Atmos. Environ. 44, 1116–1125.

Katragkou, E., Kazadzis, S., Amiridis, V., Papaioannou, V., Karathanasis, S., Melas, D., 2009. PM10 regional transport pathways in Thessaloniki, Greece. Atmos. Environ. 43, 1079–1085.

Kim, M.J., Park, R.J., Kim, J.J., 2012. Urban air quality modeling with full O3, NOx eVOC chemistry: implications for O3 and PM air quality in a street canyon. Atmos. Environ. 47, 330–340.

Kim, C.H., Park, S.Y., Kim, Y.J., Chang, L.S., Song, S.K., Moon, Y.S., Song, C.K., 2012. A numerical study on indicators of long-range transport potential for anthropogenic particulate matters over northeast Asia. Atmos. Environ. 58, 35–44.

Koçak, M., Kubilay, N., Mihalopoulos, N., 2004. Ionic composition of lower tropospheric aerosols at a Northeastern Mediterranean site: implications regarding sources and long-range transport. Atmos. Environ. 38, 2067–2077.

Leck, C., Persson, C., 1996. Seasonal and short-term variability in dimethyl sulfide, sulfur dioxide and biogenic sulfur and sea salt aerosol particles in the arctic marine boundary layer, during summer and autumn. Tellus 48B, 272–299.

Lenschow, P., Abraham, H.J., Kutzner, K., Lutz, M., PreuX, J.D., Reichenbacher, W., 2001. Some ideas about the sources of PM10. Atmos. Environ. 35 (Suppl. 1), 123–133.

Li, T.-C., Chen, W.-H., Yuan, C.-S., Wu, S.-P., Wang, X.-H., 2013. Physicochemical characteristic and source apportionment of atmospheric aerosol particles in Kimmen–Xiamen Airshed. Aerosol Air Qual. Res. 13, 308–323.

Marenco, F., Bonasoni, P., Calzolari, F., Ceriani, M., Chiari, M., Cristofanelli, P., D'Alessandro, A., Fermo, P., Lucarelli, F., Mazzei, F., Nava, S., Piazzalunga, A., Prati, P., Valli, G., Vecchi, R., 2006. Characterization of atmospheric aerosols at Monte Cimone, Italy during summer 2004: source apportionment and trans-port mechanisms. J. Geophys. Res. 111, D24202.

Masiol, M., Squizzato, S., Ceccato, D., Rampazzo, G., Pavoni, B., 2012. Determining the influence of different atmospheric circulation patterns on PM10 chemical composition in a source apportionment study. Atmos. Environ. 63, 117–124.

Meloni, D., di Sarra, A., Monteleone, F., Pace, G., Piacentino, S., Sferlazzo, D.M., 2008. Seasonal transport patterns of intense Saharan dust events at the Mediterranean Island of Lampedusa. Atmos. Res. 88, 134–148.

Moroni, B., Cappelletti, D., Marmottini, F., Scardazza, F., Ferrero, L., Bolzacchini, E., 2012. Integrated single particle-bulk chemical approach for the characterization of local and long range sources of particulate pollutants. Atmos. Environ. 50, 267–277.

Nava, S., Becagli, S., Calzolai, G., Chiari, M., Lucarelli, F., Prati, P., et al., 2012. Saharan dust impact in central Italy: an overview on three years elemental data records. Atmos. Environ. 60, 444–452.

Niemi, J.V., Saarikoski, S., Aurela, M., Tervahattu, H., Hillamo, R., Westphal, D.L., Aarnio, P., Koskentalo, T., Makkonen, U., Vehkama¨ki, H., Kulmala, M., 2009. Long-range transport episodes of fine particles in southern Finland during 1999–2007. Atmos. Environ. 43, 1255–1264.

Ohta, S., Okita, T., 1990. A chemical characterization of atmospheric aerosol in Sapporo. Atmos. Environ. 24 A, 815–822.

Pant, P., Harrison, R.M., 2012. Critical review of receptor modelling for particulate matter: a case study of India. Atmos. Environ. 49, 1–12.

Pérez, C., Nickovic, S., Baldasano, J.M., Sicard, M., Rocadenbosch, F., Cachorro, V.E., 2006a. A long Saharan dust event over the western Mediterranean: Lidar, Sun photometer observations, and regional dust modeling. J. Geophys. Res. 111, D15214.

Pérez, C., Nickovic, S., Pejanovic, G., Baldasano, J.M., Özsoy, E., 2006b. Interactive dust-radiation modeling: a step to improve weather forecasts. J. Geophys. Res. 111, D16206.

Perrino, C., Canepari, S., Catrambone, M., Dalla Torre, S., Rantica, E., Sargolini, T., 2009. Influence of natural events on the concentration and composition of atmospheric particulate matter. Atmos. Environ. 43, 4766–4779.

Putaud, J.P., Raes, F., Van-Dingenen, R., Bruggemann, E., Facchini, M.C., Decesari, S., et al., 2004. A European aerosol phenomenology-2: chemical characteristics of particulate matter at kerbside, urban, rural and back-ground sites in Europe. Atmos. Environ. 38, 2579–2595.

Querol, X., Alastuey, A., Rodríguez, S., Viana, M.M., Artíñano, B., Salvador, P., Mantilla, E., Santos, S.G.D., Patier, R.F., Rosa, J.D.L., Campa, A.S.D.L., Menéndez, M., 2004. Levels of PM in rural, urban and industrial sites in Spain. Sci. Total Environ. 334–335, 359–376.

R Development Core Team, 2013. R: A Language and Environment for Statistical Computing. the R Foundation for Statistical Computing, Vienna, Austria 3-900051-07-0 Available online at http://www.R-project.

Remoundaki, E., Bourliva, A., Kokkalis, P., Mamouri, R.E., Papayannis, A., Grigoratos, T., Samara, C., Tsezos, M., 2011. PM10 composition during an intense Saharan dust transport event over Athens (Greece). Sci. Total Environ. 409 (20), 4361–4372.

Riccio, A., Giunta, G., Chianese, E., 2007. The application of a trajectory classification procedure to interpret air pollution measurements in the urban area of Naples (Southern Italy). Sci. Total Environ. 376, 198–214.

Riccio, A., Chianese, E., Tositti, L., Baldacci, D., Sandrini, S., 2009. Modeling the transport of Saharan dust toward the Mediterranean region: an important issue for its ecological implications. Ecol. Quest. 11, 65–72.

Salvador, P., Artınano, B., Querol, X., Alastuey, A., Costoya, M., 2007. Characterisation of local and external contributions of atmospheric particulate matter at a background coastal site. Atmos. Environ. 41, 1–17.

Simon, P.K., Dasgupta, P.K., 1993. Wet effluent denuder coupled liquid/ion chromatography system. Annular and parallel plate denuders. Anal. Chem. 65, 1134–1139.

Squizzato, S., Masiol, M., Innocente, E., Pecorari, E., Rampazzo, G., Pavoni, B., 2012. A procedure to assess local and long-range transport contributions to PM2.5 and secondary inorganic aerosol. J. Aerosol Sci. 46, 64–76.

Tositti, L., Riccio, A., Sandrini, S., Brattich, E., Baldacci, D., Parmeggiani, S., Cristofanelli, P., Bonasoni, P., 2013. Short-term climatology of PM10 at a high altitude background station in southern Europe. Atmos. Environ. 65, 142–152.

Valkama, I., Kukkonen, J. (Eds.), 2004. Identification and Classification of Air Pollution Episodes in terms of Pollutants, Concentration Levels and Meteorological Conditions. Deliverable 2.1 of the FUMAPEX Project, Helsinki 30 pp.

Viana, M., Querol, X., Alastuey, A., Gil, J.I., Menéndez, M., 2006. Identification of PM sources by principal component analysis (PCA) coupled with wind direction data. Chemosphere 65 (11), 2411–2418.

Wang, Y.J., Cheng, H., Edwards, R., He, Y.Q., Kong, X.G., An, Z.S., Wu, J.Y., Kelly, I.J., Dykoski, C.A., Li, X.D., 2005. The Holocene Asian monsoon: links to solar changes and north Atlantic climate. Science 308, 854–857.

Wang, Z., Wu, T., Shi, G., Fu, X., Tian, Y., Feng, Y., Wu, X., Wu, G., Bai, Z., Zhang, W., 2012. Potential source analysis for PM10 and PM2.5 in autumn in a Northern City in China. Aerosol Air Qual. Res. 12, 39–48.